Materials Science Forum Vols. 475-479 (2005) pp 2725-2730
Online available since 2005/Jan/15 at www.scientific.net

doi:10.4028/www.scientific.net/MSF.475-479.2725

Numerical Study of the Thermal-Solutal Convection and Grain Sedimentation during Globular Equiaxed Solidification

M. Wu, A. Ludwig, J. Luo

Simulation and Modeling of Metallurical Processes
University of Leoben
Franz-Josef-Str. 18, A-8700, Leoben, Austria
Email: menghuai@notes.unileoben.ac.at

Keywords: convection, grain sedimentation, structure, macrosegregation, modeling.

Abstract. A multiphase solidification model is used to study the melt convection and grain sedimentation during globular equiaxed solidification. The melt and moving/stationary solid are treated as separated and interpenetrating phases. The transport equations (mass, momentum, enthalpy and species) for each phase, and additional scalar conservation equations necessary for description of the grain number density are solved. Six different cases including convection and grain sedimentation on an Al-4.0wt%Cu die casting are simulated and compared. Understandings to the structure and macrosegregation formation mechanisms during globular equiaxed solidification are improved.

Introduction

For a long time industry casting practice and laboratory investigations have demonstrated the importance of melt convection and grain sedimentation in solidification, structure and macrosegregation formations[1-4]. We try to use a two-phase model, developed previously[5-7], to investigate the thermo- and/or solutal convection, grain sedimentation, and their influences on the solidification and macrosegregation in the case of globular equiaxed solidification (Al-4.0 wt%Cu). The goal of this study is to achieve basic understandings to the structure and macrosegregation formation mechanisms.

Brief description of the model

The multiphase solidification problem was first modeled by Beckermann's group based on a volume-averaging approach [8-11]. This model was further modified by Ludwig and Wu for globular equiaxed solidification[5-7]. In this paper, a minor modification to the original Ludwig and Wu' model was made by using the Boussinesq approximation for the thermal-solutal convection, and gravity-induced grain sedimentation in the Navier-Stokes equations, shown as follows:

$$\frac{\partial}{\partial t}(f_l\rho_l)+\nabla\cdot(f_l\rho_l\vec{u}_l)=M_{sl} \tag{1}$$

$$\frac{\partial}{\partial t}(f_s\rho_s)+\nabla\cdot(f_s\rho_s\vec{u}_s)=M_{ls} \tag{2}$$

$$\frac{\partial}{\partial t}(f_l\rho_l\vec{u}_l)+\nabla\cdot(f_l\rho_l\vec{u}_l\otimes\vec{u}_l)=-f_l\nabla p+\nabla\cdot\bar{\bar{\tau}}_l+\vec{U}_{sl}+\vec{F}_{T-S} \tag{3}$$

$$\frac{\partial}{\partial t}(f_s\rho_s\vec{u}_s)+\nabla\cdot(f_s\rho_s\vec{u}_s\otimes\vec{u}_s)=-f_s\nabla p+\nabla\cdot\bar{\bar{\tau}}_s+\vec{U}_{ls}+\vec{F}_G \tag{4}$$

$M_{ls}(=M_{sl})$ is the mass transfer rate and $\vec{U}_{ls}(=\vec{U}_{sl})$ are momentum exchange rate between the phases. For the conservation equations Eq (1)-(4), the density in solid phase ρ_s is chosen equal to the liquid phase ρ_l. The thermal-solutal and grain sedimentation buoyancy forces are considered in the source terms ($\vec{F}_G$, $\vec{F}_{T-S}$).

$$\vec{F}_G=f_s\cdot\Delta\rho\cdot\vec{g} \tag{5}$$

$$\vec{F}_{T-S} = f_l \cdot \rho_l^{ref} \cdot \beta_T \cdot (T^{ref} - T_l) \cdot \vec{g} + f_l \cdot \rho_l^{ref} \cdot \beta_c \cdot (c^{ref} - c_l) \cdot \vec{g} \quad (6)$$

The grain number density n is also explicitly calculated by a grain transport equation[5-7]. A heterogeneous nucleation law[13-14] is implemented in the grain transport equation, and the grains are transported with the solid velocity. With the known n and f_s, the average grain size is obtained by

$$d_s = \sqrt[3]{6 f_s / (\pi n)} \quad (7)$$

With the liquid and solid concentrations, c_l and c_s, which are calculated by species conservation equations[5-7], a mixture concentration c_{mix} is defined to quantitate the macrosegregation

$$c_{mix} = \frac{c_l \cdot f_l + c_s \cdot f_s}{f_l + f_s} \quad (8)$$

Other terminologies appeared in the above equations are explained in Table I and in the previous publications [5-7].

Table I: Thermal physical and thermal dynamical parameters[5, 12]

Thermal conductivity of melt	k_l	77	W/m/K
Thermal conductivity of solid	k_s	153	W/m/K
Density of melt	ρ_l	2606	kg/m
Reference density	ρ^{ref}	2606	kg/m
Reference temperature	T^{ref}	919	K
Reference concentration	c^{ref}	0.04	/
Density difference between solid and melt	$\Delta\rho$	173	kg/m
Thermal expansion coefficient	β_T	1.0×10^{-4}	1/K
Solutal (Cu) expansion coefficient	β_c	-9.2×10^{-3}	1/wt%
Specific heat of melt	$c_{p(l)}$	1179	J/kg/K
Specific heat of solid	$c_{p(s)}$	766	J/kg/K
Latent heat of solidification	L	397000	J/kg
Viscosity of melt	μ_l	1.2×10^{-3}	kg/m/s
Diffusivity of copper in melt	D_l^{Cu}	5×10^{-9}	m^2/s
Diffusivity of copper in solid	D_s^{Cu}	8×10^{-13}	m^2/s
Melting point of pure aluminium	T_f	933.5	K
Solute partitioning coefficient	k	0.145	/
Liquidus slope	m	-3.44	K/wt%

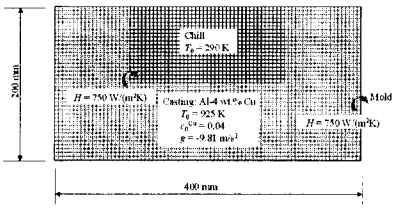

Figure 1: Configuration of the benchmark.

Table II: Case definition for the simulations

Case 1:	No convection, no grain sedimentation
Case 2:	Thermal convection only
Case 3:	Solutal convection only
Case 4:	Grain movement only
Case 5:	Thermo-solutal convection
Case 6:	Thermo-solutal convection & sedimentation

Problem description

A benchmark of an U-shape die casting (Figure 1) is simulated. The casting is assumed to be instantaneously filled with melt of a constant temperature (925 K). A steel chill is intentionally placed above the casting to enhance the cooling rate in the upper part of the casting, and hence to stress the effect of grain sedimentation. The Al-4.0wt%Cu alloy is selected because of its typical globular equiaxed solidification morphology. Six different cases are simulated and compared (Table II).

Results and discussions

Solidification sequence. The global solidification sequence is described with isolines of the fraction solid f_s. Simulation results for Case 1, 5 and 6 are compared in Figure 2. In Case 1, solidification sequence is only governed by heat transfer. The f_s isolines are identical to the isotherms. In other words, the last-to-solidify locations, namely hot spots, can be predicted purely by heat transfer calculation. In Case 5, the solidification sequence has two points different from Case 1: (i) The final solidification time (180 seconds) is shorter than that of Case 1 (223 seconds); (ii) The predicted hot spots move slightly upwards in comparison to Case 1. As a result of the melt convection, the solidification time is reduced. The upwards movement of the hot spots due to thermal-solutal convection is self-explanatory. The cold and segregated melt (rich in Cu) sinks always downwards, and the hot melt rises up. The outcome of this kind of convection is to bring heat from lower to upper regions. Due to grain sedimentation in Case 6, global solidification sequence is no longer predictable by isotherms. The grains in the upper regions, e.g. those nucleated around the chill and along the side walls, sink downwards. They sedimentate and accumulate in the lower bottom region. As the local fraction solid reaches the packing limit (0.637)[5], the solid grains settle and form a rigid porous medium. To the consequence, the last-to-solidify positions appear higher than the thermal centers in Case 1 and Case 5.

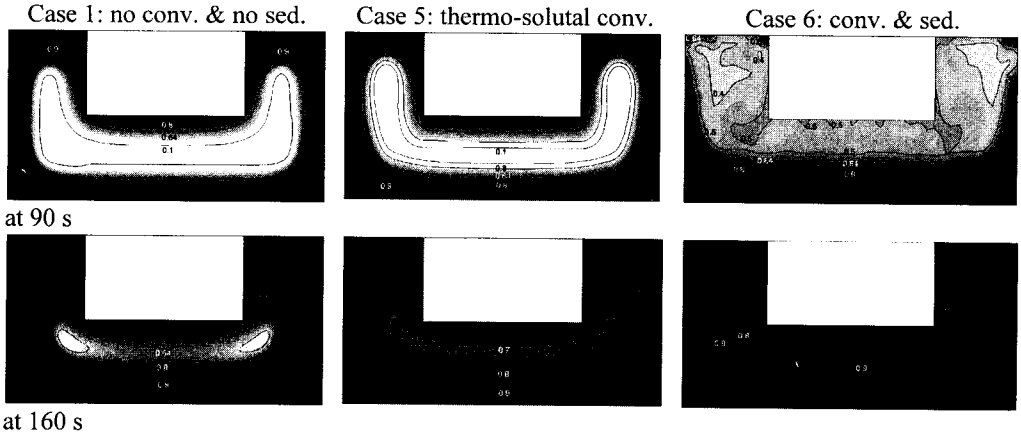

Figure 2: Influence of grain sedimentation and melt convection on the solidification sequences. The fraction solid is shown equidistantly with gray scales from zero (bright) to 1 (dark).

Thermal convection vs. solutal convection. For the Al-4%Cu alloy, the contribution of the solutal convection overweighs that of the thermal convection. As shown in Figure 3, the maximal velocity at 70 second for Case 3 is 2.45 mm/s, while it is only 0.1 mm/s for Case 2. However, similar convection patterns are achieved in both cases, because the colder melt and the melt rich in solute element (Cu) have both higher density and thus tend to sink downwards. There is always a positive temperature gradient from mold wall towards casting center. Additionally, the melt near the mold wall, when partially solidified, has always higher concentration ($k < 1$). From temperature and concentration distributions, it becomes obvious that the temperature difference between the bulk melt and the melt near the side wall is about 100 K at 70 second, while the concentration difference between the bulk melt and the melt near the mold wall is about 16 wt.%. The driving force for thermal convection $\beta_T \cdot \left(T^{ref} - T_l\right)$ is in the order of magnitude of 10^{-2}, while the driving force for solutal convection $\beta_c \cdot \left(c^{ref} - c_l\right)$ is in the order of magnitude of 10^{-1}. The convection in Case 3 is much stronger than that in Case 2. Consequently, the predicted macrosegregation in Case 3 is predicted much stronger than in Case 2.

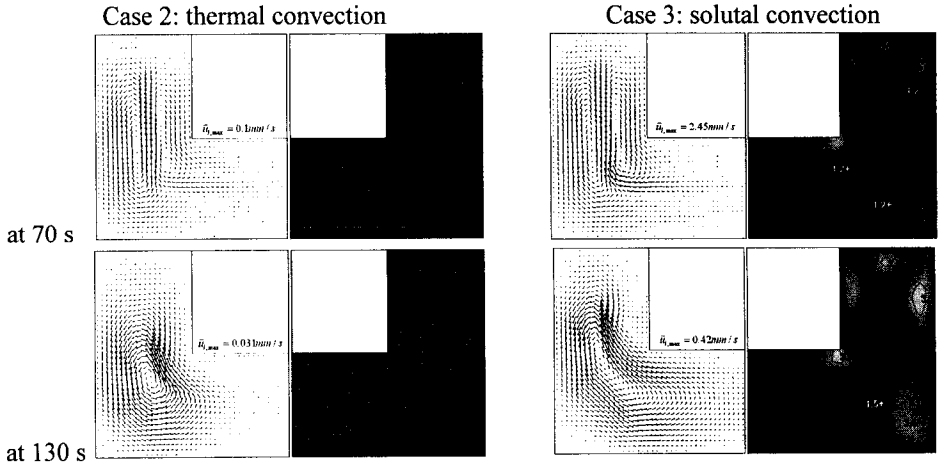

Figure 3: Comparison of thermal and solutal convection, and their influences on macrosegregations. The mixture concentration c_{mix} is scaled equidistantly by 30 gray scales from 3 wt% (bright) to 5 wt% (dark). The arrows of the melt velocity are scaled from zero to the given maximum value.

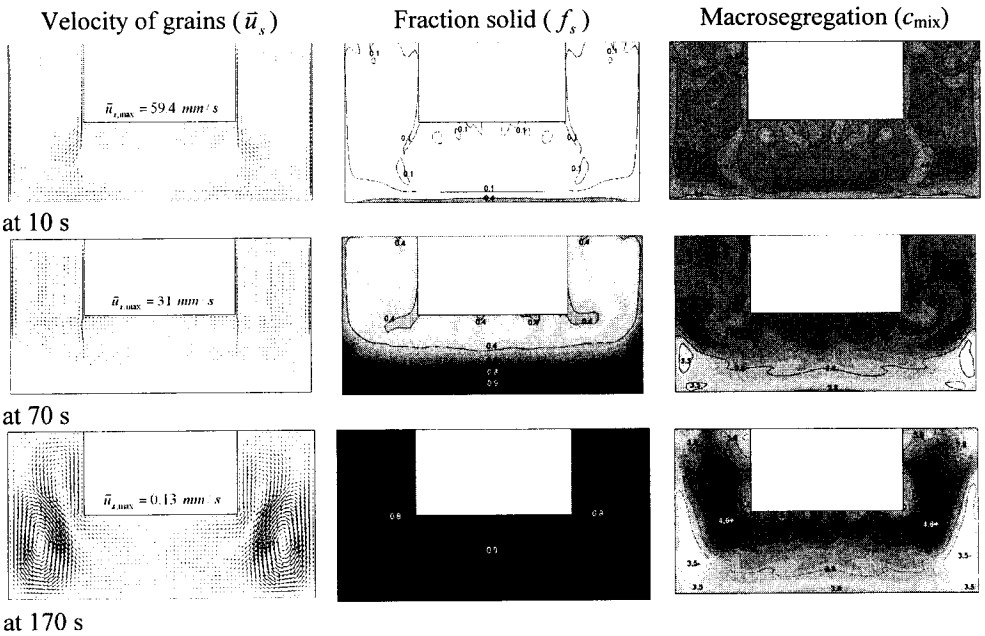

Figure 4: Macrosegregation in globular equiaxed solidification (Case 6). The c_{mix} is scaled equidistantly by 30 gray scales from 2.5 wt% (bright) to 5.5 wt%(dark), while the f_s is scaled from zero (bright) to 1 (dark). $\vec{u}_s$ is scaled from zero to the maximum value given.

Macrosegregation mechanisms. The macrosegregation formation mechanisms in Case 6 with both thermal-solutal convection and grain sedimentation are much more complicated. There are three different types of mechanisms for macrosegregations to appear: (i) grain settlement, it always results in negative segregation; (ii) depletion (leaving) of grains from a volume element, and the corresponding feed-in with segregated melt to replace the space of leaving grains, which causes

positive segregation in this volume element; and (iii) the segregated melt is squeezed out by settling grains, which causes positive segregation near the settlement region. As shown in Figure 4, the negative segregations in the bottom regions, especially near both side walls, are mainly caused by the grain settlement mechanism. Theses negative segregation zones will stay where they formed. They may become wider as solidification proceeds. The positive segregations, occurred in the early stage of solidification just above (or nearby) the settlement zones, are due to the mechanism of type (iii). Obviously, these positive segregation zones located in bulk melt move with the flow current: they are not stationary. These positive segregation zones will spread out following the flow stream. While solidification proceeds, these positive segregation zones move towards and accumulate in the last-to-solidify regions, forming a large central positive segregation zone in the final stage of solidification.

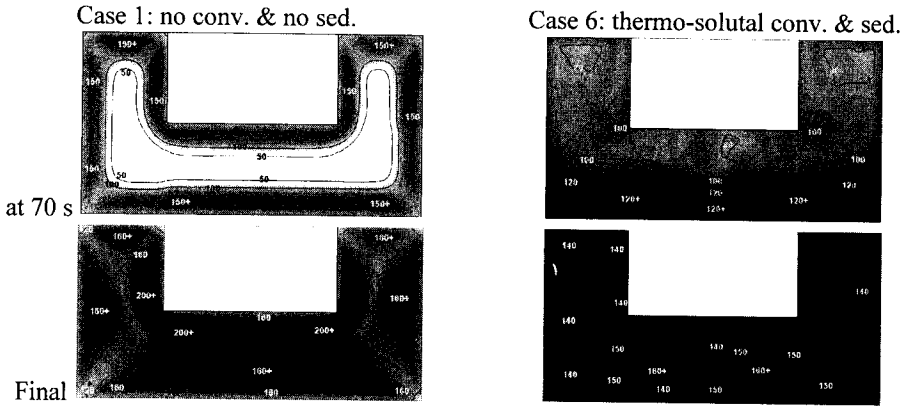

Figure 5: Grain size evaluation. The grain size is scaled equidistantly by 30 gray scales from zero (bright) to 234 μm (dark) for case 1, while from zero (bright) to 165 μm (dark) for case 6.

Grain size distribution. The Case 1 does not consider any convection and grain sedimentation. The grains stay where they nucleate. Both nucleation and grain growth depend on undercooling, or in some way on the cooling rate, but the outcomes of them are contradictory. On the one hand, the higher the cooling rate, the higher the nucleation rate, and the finer the grains should be. On the other hand, a higher cooling rate leads to higher growth rates. Predicted grain size distributions are shown in Figure 5.

There is a well-known empirical relationship[3] between the primary dendrite arm spacing λ (grain size d_s in case of equiaxed solidification) and the cooling rate $\dot{T}$, i.e. $\lambda \propto \left(\dot{T}\right)^{-n}$, where the exponent n is in the range of 1/3 to 1/2 for secondary spacings and generally very close to 1/2 for primary spacings. We calculate the criterion function $1/\sqrt{\dot{T}}$ in the same casting using the same thermal physical properties and the same boundary conditions as for Figure 2-4. The resulting grain size distribution is shown in Figure 6. It is found that the $1/\sqrt{\dot{T}}$ distribution coincides well with the predicted grain size distribution of Case 1 (Figure 5). Implications of this coincidence are: (i) the grain size distribution of Case 1 can be explained by the cooling rate through the empirical relationship $d_s \propto 1/\sqrt{\dot{T}}$; (ii) the empirical relationship between the primary dendrite arm spacing and the cooling rate may also be used to estimate the equiaxed grain size distribution for the cases no sedimentation occurs.

However, there is no coincidence between $1/\sqrt{\dot{T}}$ and the grain size distribution in Case 6 (Figure 5). The grain size distribution of Case 6 is much more uniform than Case 1. In Case 6 the grain sizes are in the range of 100 to 165 μm, while in Case 1 they are in the range of 100 to 234 μm. Relative large grains are located in the lower part of the casting.

Based on the fact that both the convection and sedimentation are sensitive to the casting geometry and process conditions, the tendency of the grain size distribution found in the presented cases does not fit to other casting geometry and boundary conditions. In order to know the effect of sedimentation on the grain size distribution in other castings individual numerical predictions are necessary.

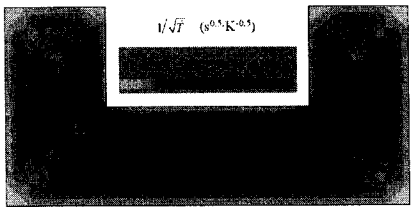

Figure 6: Calculated $1/\sqrt{\dot{T}}$ distribution in a casting ignoring both melt convection and grain sedimentation.

Conclusions

Basic understandings to the macrosegregation and grain structure formation mechanisms during globular equiaxed solidification are improved through multiphase modeling. The following basic findings are gained:

1. Effects of grain sedimentation and thermal-solutal convection cause the last-to-solidify spots to move upwards significantly. The global solidification sequence (isolines of f_s) is not simply predictable with isotherms.
2. For the Al-4.0wt%Cu alloy, the influence of solutal convection on macrosegregation overweigh that of thermal convection, but the grain sedimentation dominates both thermo- and solutal convections. Sedimentation leads to large negative segregations in the casting bottom regions, where high grain settlement rates occurs. Large positive segregation zones are predicted in the last-to-solidify regions.
3. The final grain size distribution is the joint outcome of nucleation, growth kinetics, melt convection and grain sedimentation. If ignoring the effect of the melt convection and grain segmentation, the numerically-predicted grain size distribution coincides well with that estimated by an empirical relationship ($d_s \propto 1/\sqrt{\dot{T}}$). However, in the case with grain sedimentation the grain size distribution is predicted to be much more uniform compared to the case without sedimentation.

References

[1] J. Campbell, *Castings*, (Oxford: Butterworth-Heinemann Ltd, 1991)
[2] A.Ohno, *Solidification-The Separation Theory and its Practical Applications*, (Berlin: Springer-Verlag, 1987)
[3] M.C. Flemings, *Solidification Processing*, (New York, NY: McGrow-Hill, Inc., 1974)
[4] C. Beckermann, *Intern. Mater. Rev.*, Vol 47, 2002, pp. 243-261.
[5] A. Ludwig, M. Wu, Metall. *Mater. Trans.* Vol 33A , 2002, pp. 3673.
[6] M. Wu, A. Ludwig, *Adv. Eng. Mater.*, vol. 5, 2003, pp. 62
[7] M. Wu, A. Ludwig, A. Bührig-Polaczek, M. Fehlbier, P.R. Sahm, *Int. J. Heat Mass Transfer.*, Vol 46, 2003, pp. 2819-2832
[8] J. Ni, C. Beckermann, *Metall. Trans.*, Vol 22B, 1991, pp. 349
[9] C. Beckermann and R. Viskanta, *Appl. Mech. Rev.* Vol 46, No. 1, 1993, pp.1
[10] C.Y. Wang, C. Beckermann, *Metall. Mater. Trans.*, Vol 27A, 1996, pp. 2754
[11] C. Beckermann, *Intern. Mater. Rev.*, Vol 47, 2002, pp. 243
[12] R. Trivedi, S. Liu, P. Mazumder, E. Simsek, *Sci. Techn. Adv. Mater.*, Vol 2, 2001, pp.309-320.
[13] W. Oldfield, *Trans. ASM*, Vol. 59, 1966, pp. 945-961.
[14] M. Rappaz, *Int. Mater. Rev.*, Vol. 34, 1989, pp. 93-123.

PRICM-5
doi:10.4028/www.scientific.net/MSF.475-479

Numerical Study of the Thermal-Solutal Convection and Grain Sedimentation during Globular Equiaxed Solidification

doi:10.4028/www.scientific.net/MSF.475-479.2725